# Falkland Islands Fisheries Department

## *Loligo* Stock Assessment, First Season 2015

Andreas Winter

June 2015

**Index**

**Summary**

1) The first season *Loligo* fishery of 2015 (C license) was open from February 24th to April 21st for *Loligo* target fishing. Due to a large-scale ingress of *Illex* impacting the *Loligo* stock and catches, C-license fishing after April 21st was closed north of latitude 52° S and kept open south of 52° S with the provision that vessels must switch to targeting *Illex*.

2) 19,383 tonnes of *Loligo* catch were reported in the C-license fishery through April 21st; the lowest in a 1st season since 2011. A further 41.3 tonnes *Loligo* were taken under C license after April 21st. Throughout the season 30.5% of *Loligo* catch and 28.6% of fishing effort were taken north of 52° S; 69.5% of *Loligo* catch and 71.4% of fishing effort were taken south of 52° S.

3) In the north sub-area, two immigrations / depletion periods were inferred to have started on February 26th and March 12th. In the south sub-area, four immigrations / depletion periods were inferred to have started on February 24th, March 4th, March 19th, and April 5th. Because of the exceptional influence of *Illex* on the fishery, depletion models were modified to include two selective catchability coefficients.

4) Approximately 16,026 tonnes of *Loligo* (95% confidence interval: [6,068 to 40,379] tonnes) were estimated to have immigrated into the *Loligo* Box during 1st season 2015, of which 3,615 t north of 52° S and 12,411 t south of 52° S.

5) The conservative estimate for *Loligo* remaining in the *Loligo* Box at the end of 1st season 2015 was:
Maximum likelihood of 10,194 tonnes, with a 95% confidence interval of [7,731 to 21,328] tonnes.
The risk of *Loligo* escapement biomass at the end of the season being less than 10,000 tonnes was estimated at 25.8%.

**Introduction**

The first season of the 2015 *Loligo* fishery (*Doryteuthis gahi* – Falkland calamari) opened on February 24th with 13 C-licensed vessels participating; 1 vessel took the flex option to start a day later; 2 vessels took the option to start two days later. The season was scheduled to close on April 28th (plus flex days for the late-starting vessels), one week later than the year before to enact the second phase of equalization between the 1st and 2nd season durations (Fisheries Committee, 2013). However, the ultimate extent of the season was determined by the large-scale ingress of *Illex argentinus* squid into the *Loligo* Box fishing zone. In the north sub-area of the *Loligo* Box (north of 52° S), C-license fishing was closed by emergency order at 23:59 on April 21st. In the south sub-area of the *Loligo* Box, C-license fishing was kept open from April 22nd to April 28th with the provision that vessels must switch to targeting *Illex*.

Total report *Loligo* catch under C license through April 21st was 19,383 tonnes, the lowest for a 1st season since 2011 and below median for 1st seasons since 2005 (Table 1). Additionally 41.3 tonnes *Loligo* were taken under C license after April 21st (in 80 vessel-days), when *Loligo* was effectively a bycatch species.

As in previous seasons, the *Loligo* stock assessment was conducted with depletion time-series models (Agnew et al., 1998; Roa-Ureta and Arkhipkin, 2007; Arkhipkin et al., 2008). Because *Loligo* has an annual life cycle (Patterson, 1988), stock cannot be derived from a standing biomass carried over from prior years

(Rosenberg et al., 1990). The depletion model instead calculates an estimate of population abundance over time by evaluating what levels of abundance and catchability must be extant to sustain the observed rate of catch. Depletion modelling is used both in-season and for the post-season summary, with the objective of maintaining an escapement biomass of 10,000 tonnes *Loligo* at the end of each season as a conservation threshold (Agnew et al., 2002; Barton, 2002).

Table 1. *Loligo* season comparisons since 2004. Days: total number of calendar days open to licensed *Loligo* fishing including (since 1st season 2013) optional extension days; V-Days: aggregate number of licensed *Loligo* fishing days reported by all vessels for the season.

| | Season 1 | | | Season 2 | | |
|---|---|---|---|---|---|---|
| | Catch (t) | Days | V-Days | Catch (t) | Days | V-Days |
| 2004 | | | | 17,559 | 78 | 1271 |
| 2005 | 24,605 | 45 | 576 | 29,659 | 78 | 1210 |
| 2006 | 19,056 | 50 | 704 | 23,238 | 53 | 883 |
| 2007 | 17,229 | 50 | 680 | 24,171 | 63 | 1063 |
| 2008 | 24,752 | 51 | 780 | 26,996 | 78 | 1189 |
| 2009 | 12,764 | 50 | 773 | 17,836 | 59 | 923 |
| 2010 | 28,754 | 50 | 765 | 36,993 | 78 | 1169 |
| 2011 | 15,271 | 50 | 771 | 18,725 | 70 | 1099 |
| 2012 | 34,767 | 51 | 770 | 35,026 | 78 | 1095 |
| 2013 | 19,908 | 53 | 782 | 19,614 | 78 | 1195 |
| 2014 | 28,119 | 59 | 872 | 19,630 | 71 | 1099 |
| 2015 | 19,383* | 57* | 871* | | | |

* Does not include C-license catch or effort after the C-license target for that season was switched from *Loligo* to *Illex*.

**Methods**

The depletion model formulated for the Falkland Islands *Loligo* stock is based on the equivalence:

$$C_{day} = q \times E_{day} \times N_{day} \times e^{-M/2} \tag{1}$$

where q is the catchability coefficient, M is the natural mortality rate (considered constant at 0.0133 day$^{-1}$; Roa-Ureta and Arkhipkin, 2007), and $C_{day}$, $E_{day}$, $N_{day}$ are catch (numbers of *Loligo*), fishing effort (numbers of vessels), and abundance (numbers of *Loligo*) per day. In its basic form (DeLury, 1947) the depletion model assumes a closed population in a fixed area for the duration of the assessment. However, the assumption of a closed population is imperfectly met in the Falkland Islands fishery, where stock analyses have often shown that *Loligo* groups arrive in successive waves after the start of the season (Roa-Ureta, 2012; Winter and Arkhipkin, 2012). Arrivals of successive groups are inferred from discontinuities in the catch data. Fishing on a single, closed cohort would be expected to yield gradually decreasing CPUE, but gradually increasing average individual sizes, as the squid grow. When instead these data change suddenly, or in contrast to expectation, the immigration of a new group to the population is indicated.
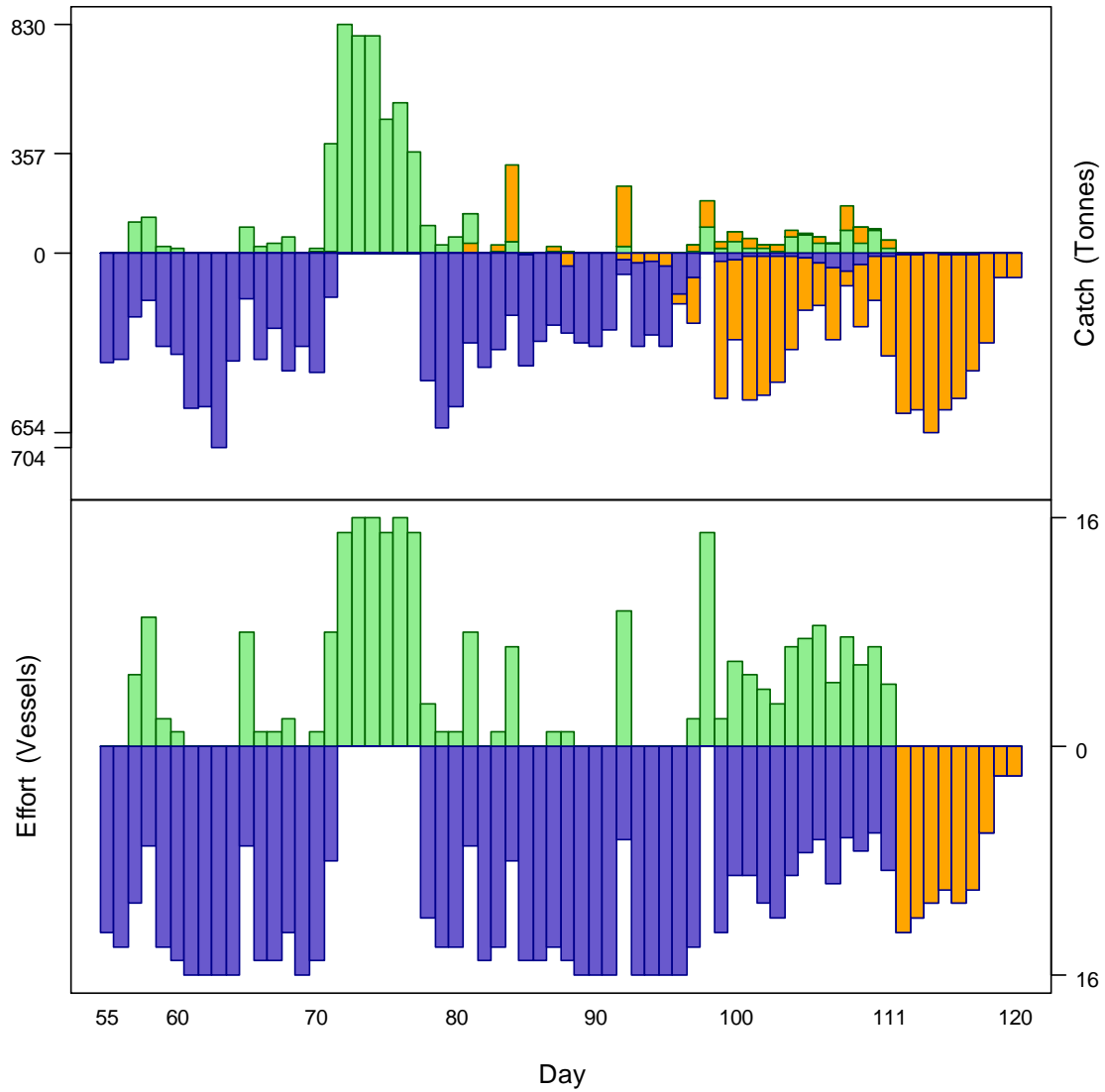
Figure 1. Daily total *Loligo* catch and effort distribution by assessment sub-area north (green) and south (purple) of 52º S in the C license season 2015. Orange shows *Illex* catch and effort. The season was open for *Loligo* target from February 24th (day 55) to April 21st (day 111), then open in the south only for *Illex* target to April 28th (day 118); 2 vessels fished flex days until April 30th (day 120). As many as 16 vessels fished per day north of 52º S; as many as 16 vessels fished per day south of 52º S. As much as 830 tonnes *Loligo* was caught per day north of 52º S; as much as 704 tonnes *Loligo* was caught per day south of 52º S. As much as 357 tonnes *Illex* was caught per day north of 52º S; as much as 654 tonnes *Illex* was caught per day south of 52º S.

In the event of a new group arrival, the depletion calculation must be modified to account for this influx. This was done using a simultaneous algorithm (Roa-Ureta, 2012) that adds new arrivals on top of the stock previously present, and posits a common catchability coefficient for the entire depletion time-series. If two depletions are included in the same model (i.e., the stock present from the start plus a new group arrival), then:

$$C_{day} = q \times E_{day} \times (N1_{day} + (N2_{day} \times i2 \big|_0^1)) \times e^{-M/2} \qquad \textbf{(2)}$$

where i2 is a dummy variable taking the values 0 or 1 if 'day' is before or after the start day of the second depletion. For more than two depletions, $N3_{day}$, i3, $N4_{day}$, i4, etc., would be included following the same pattern.

Further modification of the depletion model was imposed this season by the large-scale ingress of *Illex* into the *Loligo* Box. The inter-specific dynamics between *Loligo* and *Illex* (Arkhipkin and Middleton, 2002a) are likely to alter the population status of *Loligo* under these conditions, and the rapid increase in *Illex* catches part-way through the season (Figure 1) confounded the assumption of a closed population, just as new group arrivals do. During the 1st *Loligo* season of 2011 high *Illex* catches occurred over several days in the north (Winter, 2011). The inference was made in that season that vessels with high *Illex* catch proportions were actively targeting *Illex*, and the depletion model was modified by adjusting any vessel's 'effort-day' downward as a fractional value equivalent to the ratio between *Loligo* and *Illex* catch for that vessel on that day. The same type of effort adjustment was initially tried for the current season, but following the consistent predominance of *Illex* catches by all vessels over multiple days a more precise approach was implemented. Two catchability coefficients q instead of one were included in the depletion model, applicable to days of respectively high and low *Illex* proportions in the catch:

$$C_{day} \qquad = q_{day}\Big|_{lo\ Illex}^{hi\ Illex} \times E_{day} \times (N1_{day} + (N2_{day} \times i2\big|_{0}^{1})) \times e^{-M/2} \qquad \textbf{(3)}$$

Both catchability coefficients $q_{lo\ Illex}$ and $q_{hi\ Illex}$ were free parameters in the model, as was the switch between them; i.e., the model itself selected the optimum threshold of what proportion of *Illex* in the catch triggered a different catchability. It is noted that this represents an empirical extension to the model; there is no intrinsic reason why the system would now have exactly two catchability rates and not three or more. However, the decision was made to keep the model as simple as possible while still addressing the changes caused by the ingress of *Illex*. The depletion model was calculated with data only to the extent of the season that was allocated to targeting *Loligo* (April 21st; see Introduction), but the parameter predictions were then extended to the end of the full season, April 30th.

The *Loligo* stock assessment was calculated in a Bayesian framework (Punt and Hilborn, 1997), whereby results of the season depletion model are conditioned by prior information on the stock; in this case the information from the pre-season survey. The season depletion likelihood function was calculated as the difference between actual catch numbers reported and catch numbers predicted from the model (equation **3**), statistically corrected by a factor relating to the number of days of the depletion period (Roa-Ureta, 2012):

$$((n\text{Days} - 2)/2) \times \log\left(\sum_{days}\left(\log(\text{predicted } C_{day}) - \log(\text{actual } C_{day})\right)^2\right) \qquad \textbf{(4)}$$

The survey prior likelihood function was calculated as the normal distribution of the difference between catchability (q) derived from the survey abundance estimate, and catchability derived from the season depletion model. For equation **5** the 'lo *Illex*' catchability was used (i.e., $q_{model} = q_{lo\ Illex}$), because the season started with low levels of *Illex* catch:

$$\frac{1}{\sqrt{2\pi \cdot SD_{q\,survey}^{2}}} \times exp\left(-\frac{\left(q_{model} - q_{survey}\right)^{2}}{2 \cdot SD_{q\,survey}^{2}}\right) \tag{5}$$

Catchability, rather than abundance N, was used for calculating the survey prior likelihood because catchability informs the entire season time series; whereas N from the survey only informs the initial season depletion period – subsequent immigrations and depletions are independent of the abundance that was present during the survey.

Bayesian optimization of the depletion was calculated by jointly minimizing equations **4** and **5**, using the Nelder-Mead algorithm in R programming package 'optimx' (Nash and Varadhan, 2011). Relative weights in the joint optimization were assigned to equations **4** and **5** as the converse of their coefficients of variation (CV), i.e., the CV of the prior became the weight of the depletion model and the CV of the depletion model became the weight of the prior. Calculations of the CVs are described in the Appendix.

With $C_{day}$, $E_{day}$ and M being fixed parameters, the optimization of equation **3** using equations **4** and **5** produces estimates of $q_{lo\,Illex}$, $q_{hi\,Illex}$ and N1, N2, …, etc. Numbers of *Loligo* on the final day (or any other day) of a time series are then calculated as the numbers N of the depletion start days discounted for natural mortality during the intervening period, and subtracting cumulative catch also discounted for natural mortality (CNMD). Taking for example a two-depletion period:

$$
\begin{aligned}
N_{final\,day} \quad = \quad & N1_{start\,day\,1} \times e^{-M\,(final\,day\,-\,start\,day\,1)} \\
+ \, & N2_{start\,day\,2} \times e^{-M\,(final\,day\,-\,start\,day\,2)} \\
- \, & CNMD_{final\,day}
\end{aligned} \tag{6}
$$

where

$$CNMD_{day\,1} \quad = \quad 0$$

$$CNMD_{day\,i} \quad = \quad CNMD_{day\,i-1} \times e^{-M} + C_{day\,i-1} \times e^{-M/2} \tag{7}$$

$N_{final\,day}$ (or any other day) is then multiplied by the average individual weight of *Loligo* on that day to give biomass. Daily average individual weight was obtained from length / weight conversion of mantle lengths measured in-season by observers, and also derived from in-season commercial data as the proportion of product weight that vessels reported per market size category. Observer mantle lengths are scientifically precise, but restricted to 1-2 vessels at any one time that may or may not be representative of the entire fleet. Commercially proportioned mantle lengths are relatively less precise, but cover the entire fishing fleet. Therefore, both sources of data were used. Daily average individual weights were calculated by averaging observer size samples and commercial size categories on days when observer data were available, otherwise only commercial size categories. When available, the observer data were always weighted as half of the average, irrespective of how many vessels provided commercial size categories that day. To smooth fluctuations, the expected value of the daily average individual weight was taken from its GAM trend (see Appendix) rather than the empirical value on each day.

Distributions of the likelihood estimates from joint optimization (i.e., measures of their statistical uncertainty) were computed using a Markov Chain Monte Carlo (MCMC) (Gamerman and Lopes, 2006), a method that is commonly employed

for fisheries assessments (Magnusson et al., 2013). MCMC is an iterative process which generates random stepwise changes to the proposed outcome of a model (in this case, the N and q of *Loligo*, as well as to the switch proportion between lo and hi q) and at each step, accepts or nullifies the change with a probability equivalent to how well the change fits the model parameters compared to the previous step. The resulting sequence of accepted or nullified changes (i.e., the 'chain') approximates the likelihood distribution of the model outcome. The MCMC of the depletion models were run for 200,000 iterations; the first 1000 iterations were discarded as burn-in sections (initial phases over which the algorithm stabilizes); and the chains were thinned by a factor equivalent to the maximum of either 5 or the inverse of the acceptance rate (e.g., if the acceptance rate was 12.5%, then every $8^{th}$ ($0.125^{-1}$) iteration was retained) to reduce serial correlation. For each model three chains were run; one chain initiated with the parameter values obtained from the joint optimization of equations **4** and **5**, one chain initiated with these parameters ×2, and one chain initiated with these parameters ×¼. Convergence of the three chains was accepted if the variance among chains was less than 10% higher than the variance within chains (Brooks and Gelman, 1998). When convergence was satisfied the three chains were combined as one final set. Equations **6**, **7**, and the multiplication by average individual weight were applied to CNMD and each MCMC iteration of N values in the final set, and the biomass outcomes from these calculations represent the distribution of the estimate.

Total escapement biomass is defined as the aggregate biomass of *Loligo* on the last day of the season for north and south sub-areas combined. *Loligo* sub-stocks emigrate from different spawning grounds and remain to an extent segregated (Arkhipkin and Middleton, 2002b). However, it is not assumed that north and south biomasses are uncorrelated (Shaw et al., 2004), and therefore north and south likelihood distributions were added semi-randomly in proportion to the strength of their day-to-day correlation. The semi-randomization is described in the Appendix.


**Stock assessment**
**Data**

*Loligo* catch and fishing effort were strongly segregated between the south and north, typical of recent $1^{st}$ seasons (compare Figure 2 with Winter, 2013; 2014). 30.5% of *Loligo* catch and 28.6% of effort were taken north of 52º S. 68.3% of *Loligo* catch and 67.6% of effort were taken south of 52º S and west of 58.5º W; just 1.1% of *Loligo* catch and 3.8% of effort were taken south of 52º S and east of 58.5º W.

A total of 951 vessel-days were fished during the season, 871 days targeting *Loligo* with a median of 15 vessels fishing per calendar day (Figure 1), and 80 days targeting *Illex* with a median of 11 vessels fishing per calendar day (although this includes the flex days for the late-starting vessels, which by default were pushed into the *Illex* allocation). Vessels reported daily catch totals to the FIFD and electronic logbook data that included trawl times, positions, and product weight by market size categories. Two FIFD observers were deployed on three vessels in the fishery for a total of 67 observer-days, of which all except 1 before the target allocation was switched from *Loligo* to *Illex*. Throughout the 57 days of the *Loligo* target season, 3 days had no observer covering, 42 days had 1 observer covering, and 12 days had two observers covering. Observers sampled an average of 410.9 *Loligo* daily, and reported their maturity stages, sex, and lengths to 0.5 cm. The length-weight relationship for

converting both observer and commercially proportioned length data was taken from the pre-season survey (Winter et al, 2015):

$$\text{weight (kg)} \quad = \quad 0.128 \times \text{length (cm)}^{2.347} / 1000 \qquad \textbf{(8)}$$
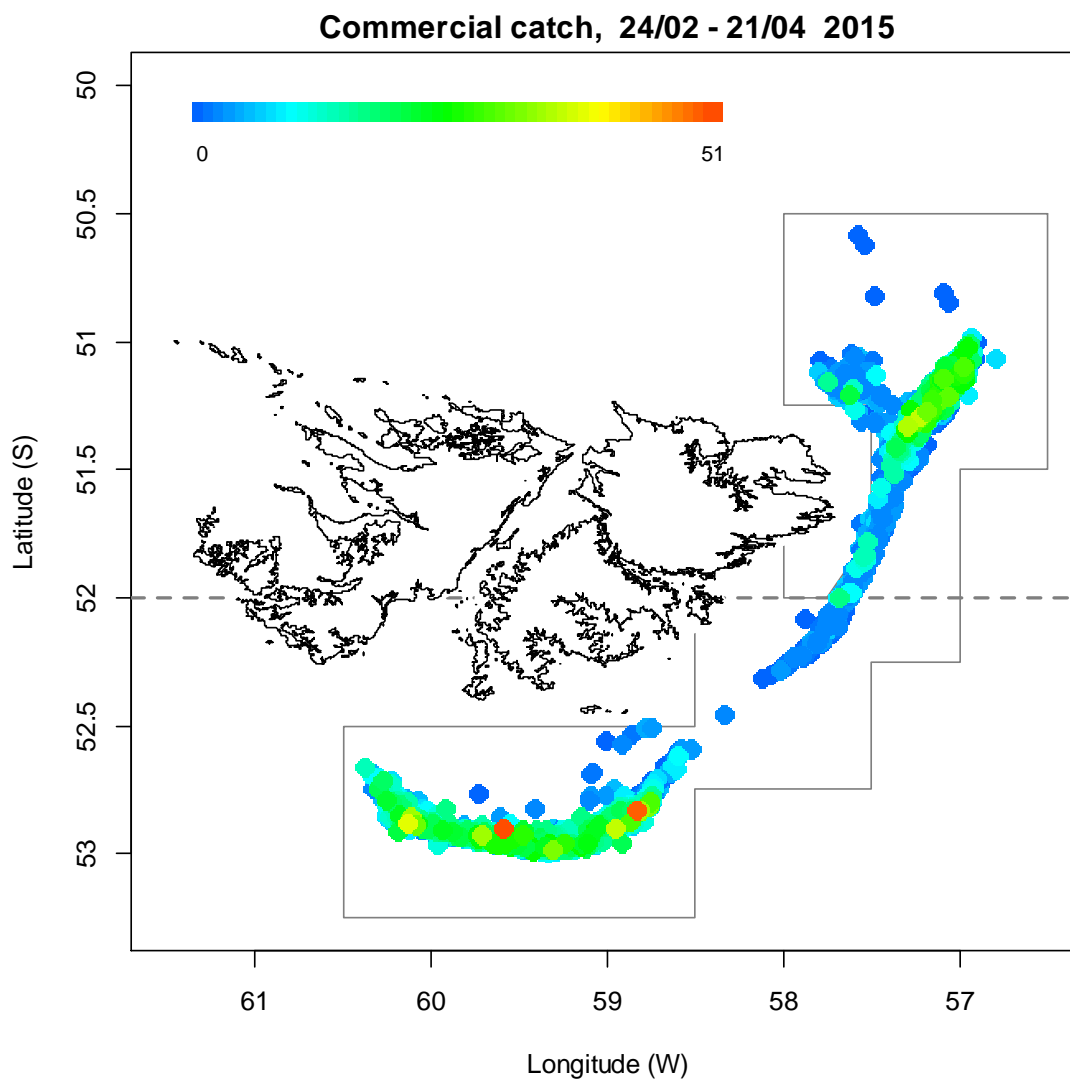
**Commercial catch, 24/02 - 21/04 2015**



Figure 2. Spatial distribution of *Loligo* 1st-season commercial catches, colour-scaled to catch weight (max. = 51 t). 2575 trawl catches were taken during the season (excluding catches taken after C license target allocation was switched to *Illex*). The 'Loligo Box' fishing zone, and the 52 ºS parallel delineating north and south assessment sub-areas, are shown in gray.

## Group arrivals / depletion criteria

Start days of depletions - following arrivals of new *Loligo* groups - were judged primarily with reference to daily changes in CPUE, with additional information from sex proportions, maturity, and average individual *Loligo* sizes. CPUE was calculated as metric tonnes of *Loligo* caught per vessel per day. Days were used rather than trawl

hours as the basic unit of effort. Commercial vessels do not trawl standardized duration hours, but rather durations that best suit their daily processing requirements. An effort index of days is therefore more consistent.

Two days in the north and four days in the south were identified that represented the onset of separate immigrations / depletions in the season.

- The first depletion north was identified on day 57 (February 26th – two days past the start of the commercial season), which represented the first day of commercial effort in the north and the highest CPUE in the north for the next 9 days (Figure 3).
- The second depletion north was identified on day 71 (March 12th) with a strong CPUE increase (Figure 3), and the day after a local minimum in average commercial weight (Figure 4A).
- The first depletion south was identified on day 55 (February 24th – the start of the commercial season) with 13 vessels starting the fishery in the south (Figure 1) and the highest CPUE for the next 5 days (Figure 3).
- The second depletion south was identified on day 63 (March 4th) with a CPUE peak that was the highest for the next 15 days (Figure 3), and local minima in average commercial weights and observer weights (Figure 4A & B).
- The third depletion south was identified on day 78 (March 19th) with the resumption of commercial fishing in the south after an absence of 6 days (Figure 1). CPUE was the highest since the previous depletion start (day 63) (Figure 3). Average maturities had generally increasing trends although it cannot be ascertained that day 78 represented the start date of the increase (Figure 4D).
- The fourth depletion south was identified on day 95 (April 5th). CPUE reached a small peak (Figure 3). Average commercial weights, average observer weights, female proportion, and average maturities all presented local minima (Figure 4A, B, C & D).
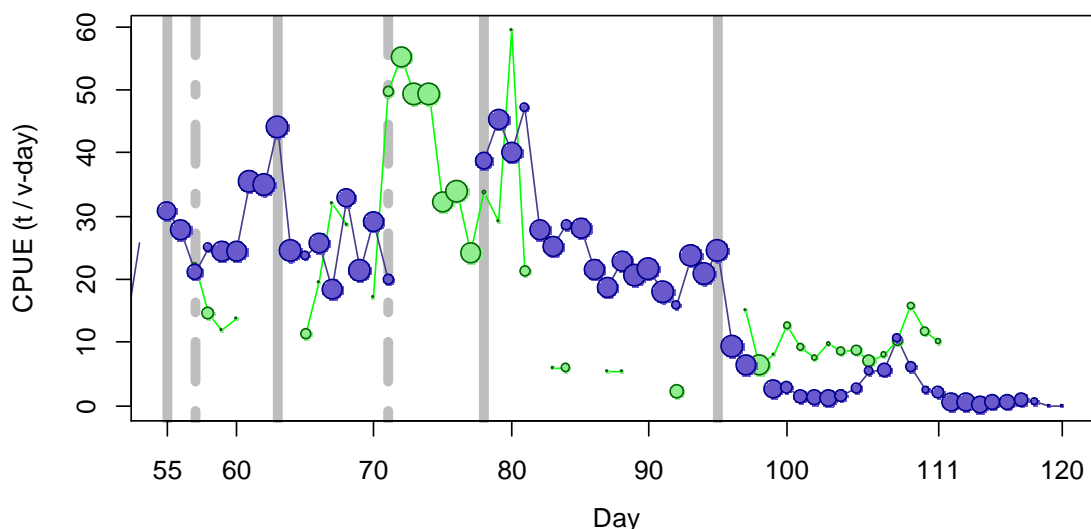


Figure 3. CPUE in metric tonnes per vessel per day, by assessment sub-area north (green) and south (purple) of the 52º S parallel. Circle sizes are proportioned to the numbers of vessel fishing. Data from consecutive days are joined by line segments. Broken gray bars indicate days 57 and 71, identified as the start of in-season depletions north. Solid gray bars indicate days 55, 63, 78 and 95, identified as the start of in-season depletions south.
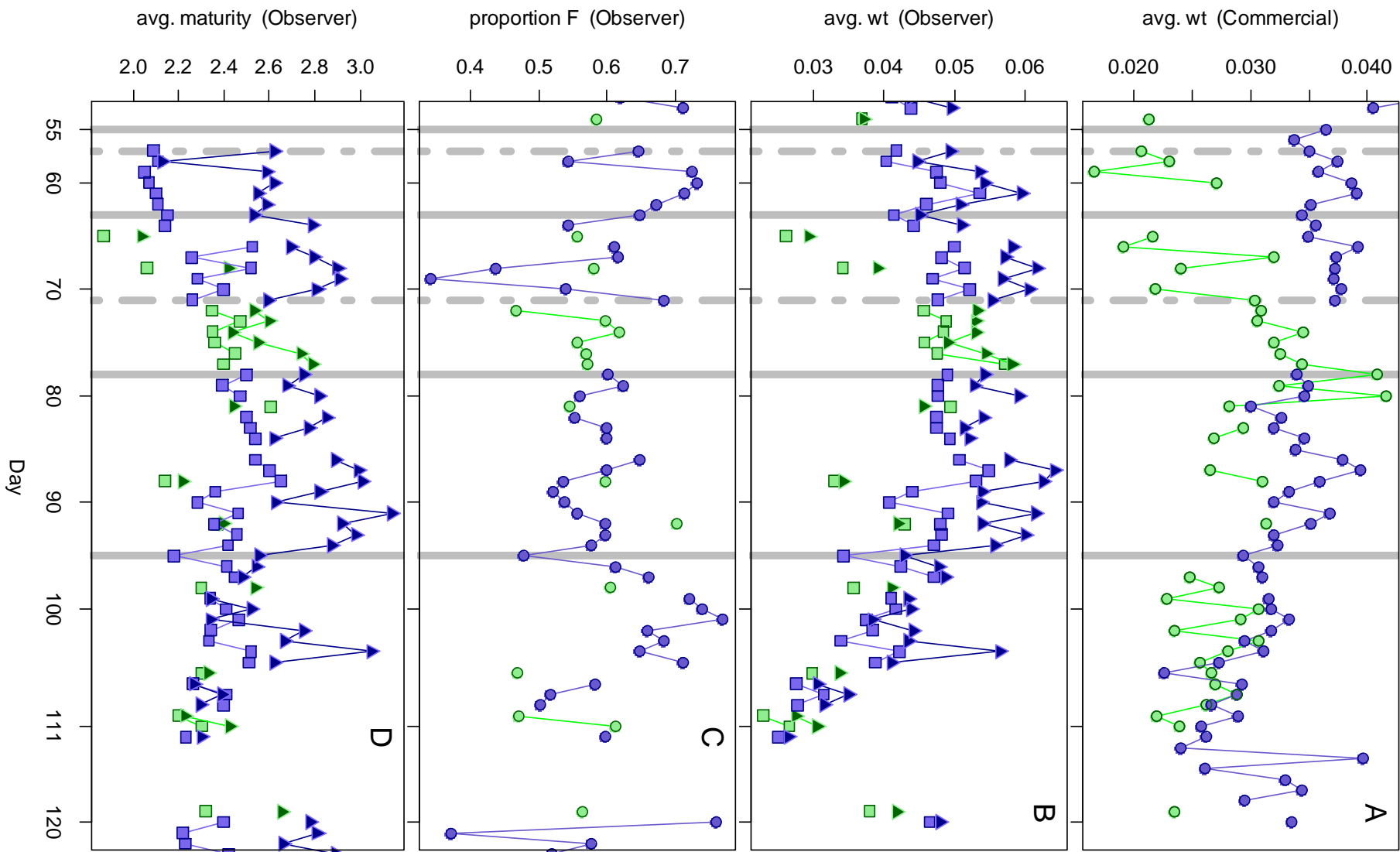
10

Figure 4 [previous page]. A: Avg. individual *Loligo* weights (kg) per day from commercial size categories. B: Avg. individual *Loligo* weights (kg) by sex per day from observer samples. C: Proportions of female *Loligo* per day from observer samples. D: avg. maturity value by sex per day from observer samples. In all graphs – Males: triangles, females: squares, unsexed: circles. North: green, south: purple. Consecutive days are joined by line segments. Broken gray bars indicate days 57 and 71, identified as the start of in-season depletions north. Solid gray bars indicate days 55, 63, 78 and 95, identified as the start of in-season depletions south.

## Depletion analyses
## South

The complex structure of this season's depletion modelling resulted in Bayesian posterior optimization on initial catchability ($q_{lo\ Illex}$; Figure 5-left) that was predominantly driven by the pre-season prior: maximum likelihood $_{Bayesian} q_{S\ lo\ Illex} = 1.114 \times 10^{-3}$ (equation **A10-S**), from $_{prior} q_S = 1.058 \times 10^{-3}$ (equation **A4-S**) and $_{depletion} q_S = 3.166 \times 10^{-3}$; (equation **A6-S**). Respective weights in the Bayesian optimization (converse of the CVs) were 0.465 for the in-season depletion (**A5-S**) and 0.404 for the prior (**A9-S**).
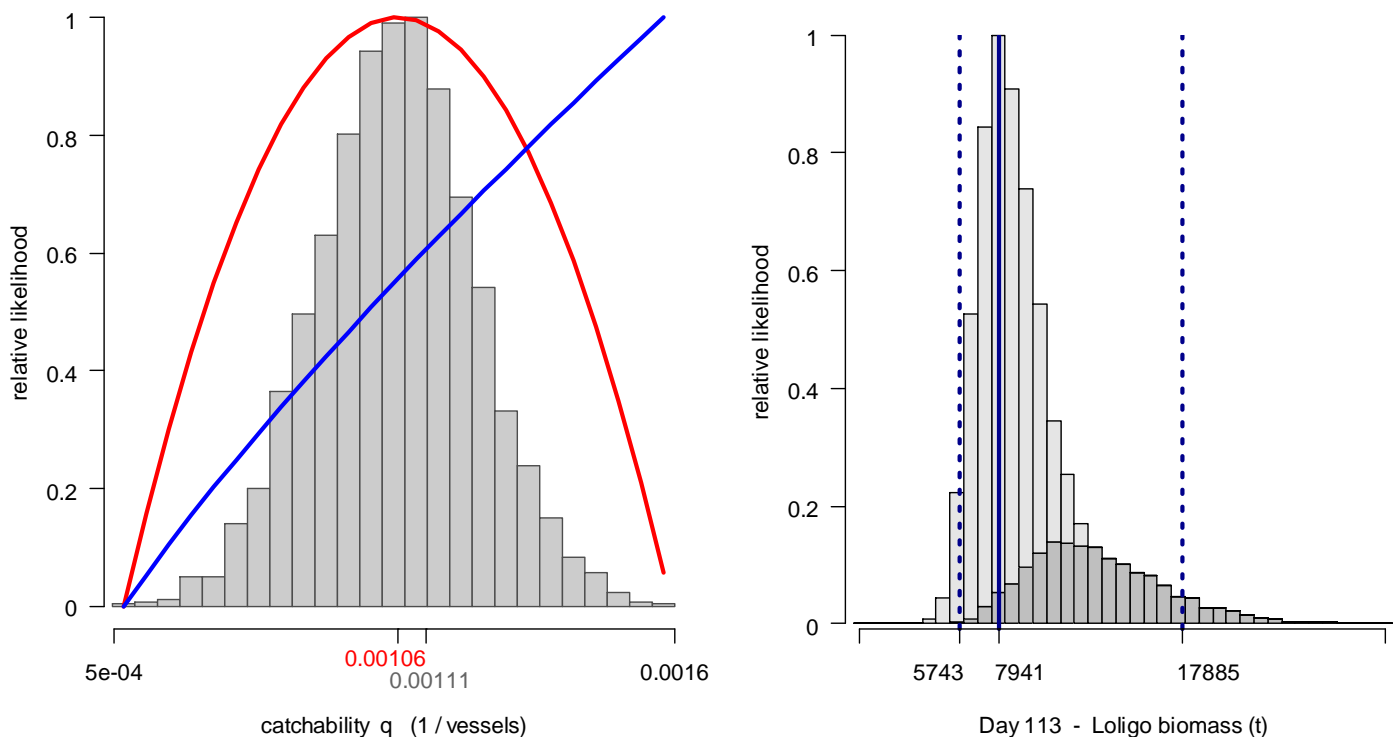


Figure 5. South sub-area. Left: Likelihood distributions for *Loligo* initial catchability. Red line: prior model (pre-season survey), blue line: in-season depletion model, gray bars: MCMC iterations of the combined Bayesian posterior model. Right: Likelihood distribution of biomass on day 113, from Bayesian posterior and avg. individual *Loligo* weight. Blue lines: maximum likelihood and 95% confidence interval. Note the correspondence to Figure 6.

The MCMC distribution of the Bayesian posterior multiplied by the GAM fit of average individual *Loligo* weight (Figure A1-south) gave the likelihood distribution

of *Loligo* biomass on day 113 (April 23$^{rd}$) shown in Figure 5-right, with maximum likelihood and 95% confidence interval of:

$$B_{S\ day\ 113} = 7,941\ t \sim 95\%\ CI\ [5,743 - 17,885]\ t \qquad \textbf{(9)}$$

The two gray tones on the bar plot represent two modes caused by the selective application of two catchability coefficients q. The depletion model optimization and most MCMC iterations clustered near a q switch of 0.907 (equation **A10-S**), meaning that the algorithm would switch from $q_{lo\ Illex}$ to $q_{hi\ Illex}$ on days when *Illex* catch was ≥90.7% of the total squid catch. However, 21% of MCMC iterations accepted a q switch lower than 0.82 (Figure A3-S). Taking 0.82 as the break-point (by eye), Figure 5-right shows a secondary mode of MCMC outcomes (darker gray) that would centre the likelihood of $B_{S\ day\ 113}$ at around 11,000 t.
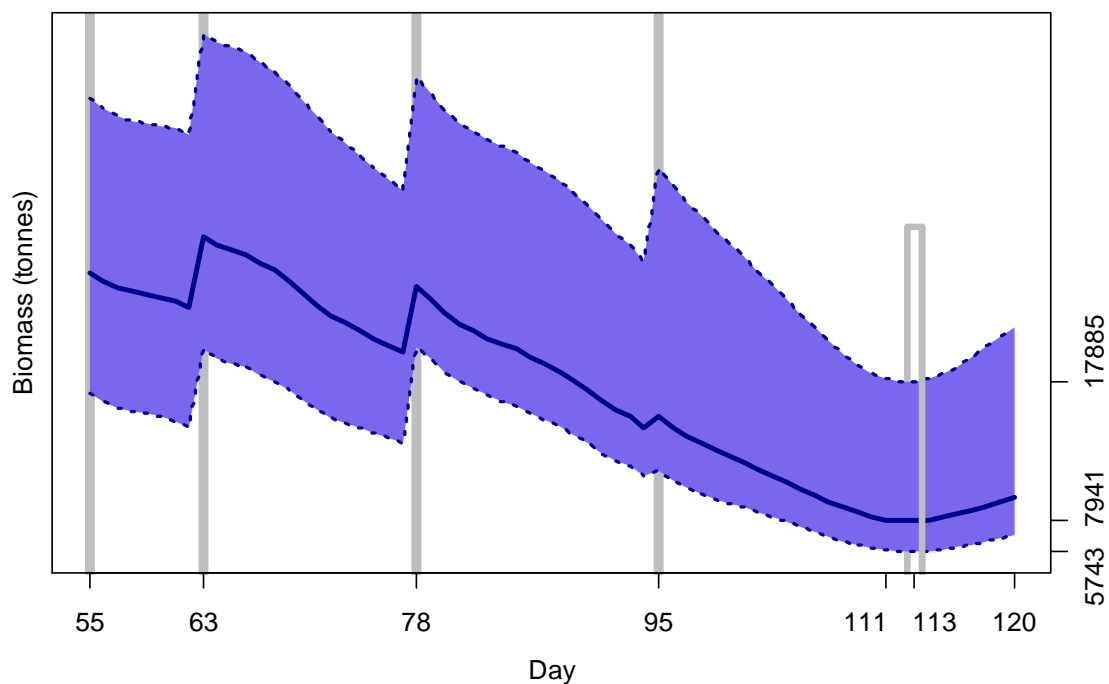


Figure 6. South sub-area *Loligo* biomass time series estimated from Bayesian posterior of the depletion model ± 95% confidence intervals. Solid gray bars indicate days 55, 63, 78 and 95, identified as the start of in-season depletions south. Note that the biomass 'footprint' on day 113 corresponds to the right-side plot of Figure 5.

Day 113 was represented for this calculation rather than day 120 (April 30$^{th}$), the final day of the season, because *Loligo* biomass estimated from the depletion model time series reached a minimum on day 113 before increasing over the last week of the season (Figure 6)$^A$. The increase of the last week was ascribed to an artefact. The average individual weight trend of *Loligo* showed a significant increase in the last week (Figure A1-south). That average individual weight increase was likely due to the fishery having switched to targeting *Illex*, whereby most *Loligo* still being caught in the fishery thereafter were selectively larger ones capable of surviving in the

---

$^A$ As the South had most of the catch overall (see Data section), this minimum day for the South was also the minimum for the total.

presence of *Illex*. However, as the depletion model itself was only optimized to the end of *Loligo*-target fishing on April 21$^{st}$ (see Methods), the subsequent increase in average individual weight was not compensated in the depletion model and resulted in an apparent increasing trend of biomass. The more plausible season-end biomass was therefore conservatively taken as the minimum biomass on day 113.

**North**

In the north sub-area, Bayesian optimization on initial catchability ($q_{lo\ Illex}$; Figure 7-left) was also predominantly driven by the pre-season prior: maximum likelihood $_{Bayesian}q_{N\ lo\ Illex} = 3.306 \times 10^{-3}$ (equation **A10-N**), from $_{prior}q_N = 3.300 \times 10^{-3}$ (equation **A4-N**) and $_{depletion}q_N = 2.037 \times 10^{-3}$; (equation **A6-N**). Respective weights in the Bayesian optimization (converse of the CVs) were 0.555 for the in-season depletion (**A5-N**) and 0.719 for the prior (**A9-N**).
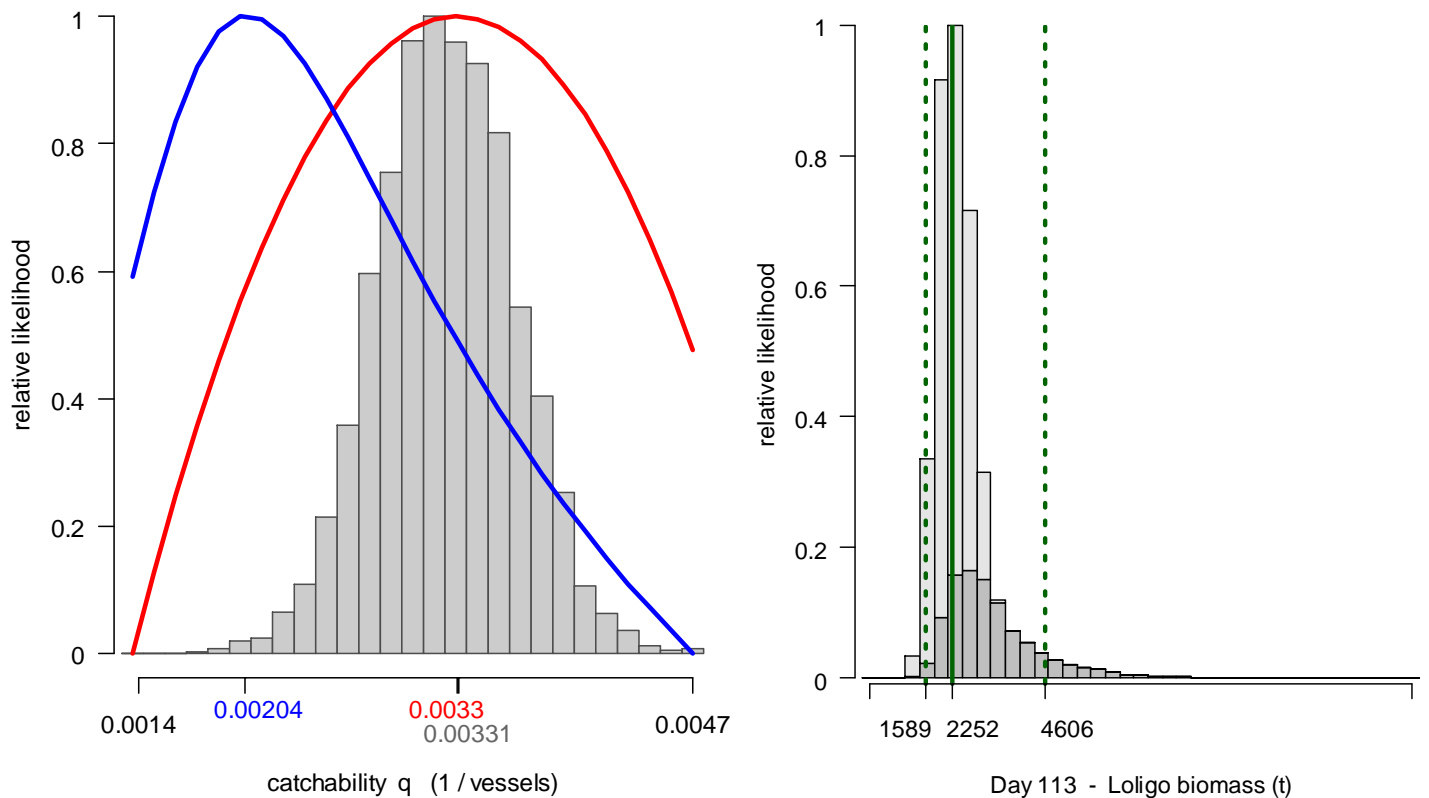


Figure 7. North sub-area. Left: Likelihood distributions for *Loligo* catchability. Red line: prior model (pre-season survey), blue line: in-season depletion model, gray bars: MCMC iterations of the combined Bayesian posterior model. Right: Likelihood distribution of biomass on day 113, from Bayesian posterior and average individual *Loligo* weight on that date. Green lines: maximum likelihood and 95% confidence interval. Note the correspondence to Figure 8.

The MCMC distribution of the Bayesian posterior multiplied by the GAM fit of average individual *Loligo* weight (Figure A1-north) gave the likelihood distribution of *Loligo* biomass on day 113 (April 23$^{rd}$) shown in Figure 7-right, with maximum likelihood and 95% confidence interval of:

$$B_{N\,day\,113} \qquad = \quad 2{,}252 \text{ t} \sim 95\% \text{ CI } [1{,}589 - 4{,}606] \text{ t} \qquad\qquad \textbf{(10)}$$

The two gray tones on the bar plot again represent two modes caused by selective application of two catchability coefficients q. The depletion model optimization and most MCMC iterations clustered near q switch $_N$ = 0.818, but 22% of MCMC iterations accepted a q switch lower than 0.74 (Figure A3-N). Taking 0.74 as the break-point, Figure 7-right shows a secondary mode of MCMC outcomes (darker gray) that would centre the likelihood of $B_{N\,day\,113}$ slightly higher at around 2,750 t.

Day 113 was taken as the nominal season-end date for equivalence with the south sub-area. However in the north, the depletion model biomass estimate decreased continuously to the last day of the season, day 120 - April 30th (Figure 8).
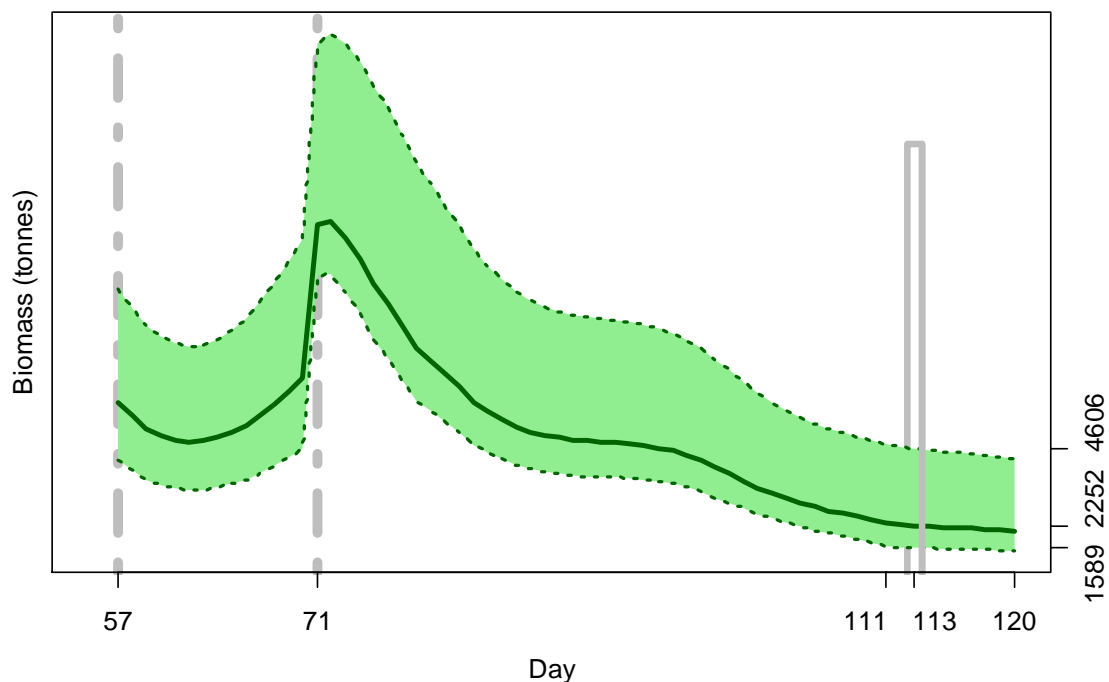


Figure 8. North sub-area *Loligo* biomass time series estimated from Bayesian posterior of the depletion model ± 95% confidence intervals. Broken gray bars indicate days 57 and 71, identified as the start of in-season depletions north. Note that the biomass 'footprint' on day 113 corresponds to the right-side plot of Figure 7.

**Escapement biomass**

Total escapement biomass was defined as the aggregate biomass of *Loligo* on day 113 (April 23rd) for north and south sub-areas combined (equations **9** and **10**).

$$B_{Total\,day\,120} \qquad = \quad B_{N\,day\,120} \; + \; B_{S\,day\,120}$$
$$\qquad\qquad\qquad = \quad 10{,}194 \text{ t} \sim 95\% \text{ CI } [7{,}731 - 21{,}328] \text{ t} \qquad \textbf{(11)}$$

As for the north and south sub-areas separately, the combined escapement distribution comprised a higher, secondary mode of escapement biomass maximum likelihood; centred at around 15,000 tonnes and corresponding to alternate levels of the q

switches. Semi-randomized addition of the north and south biomass estimates gave the aggregate likelihood distribution of total escapement biomass shown in Figure 9.

The risk of the fishery, defined as the proportion of the total escapement biomass distribution below the conservation limit of 10,000 tonnes (Agnew et al., 2002; Barton, 2002), was calculated as 25.8% (white shading lines on Figure 9).
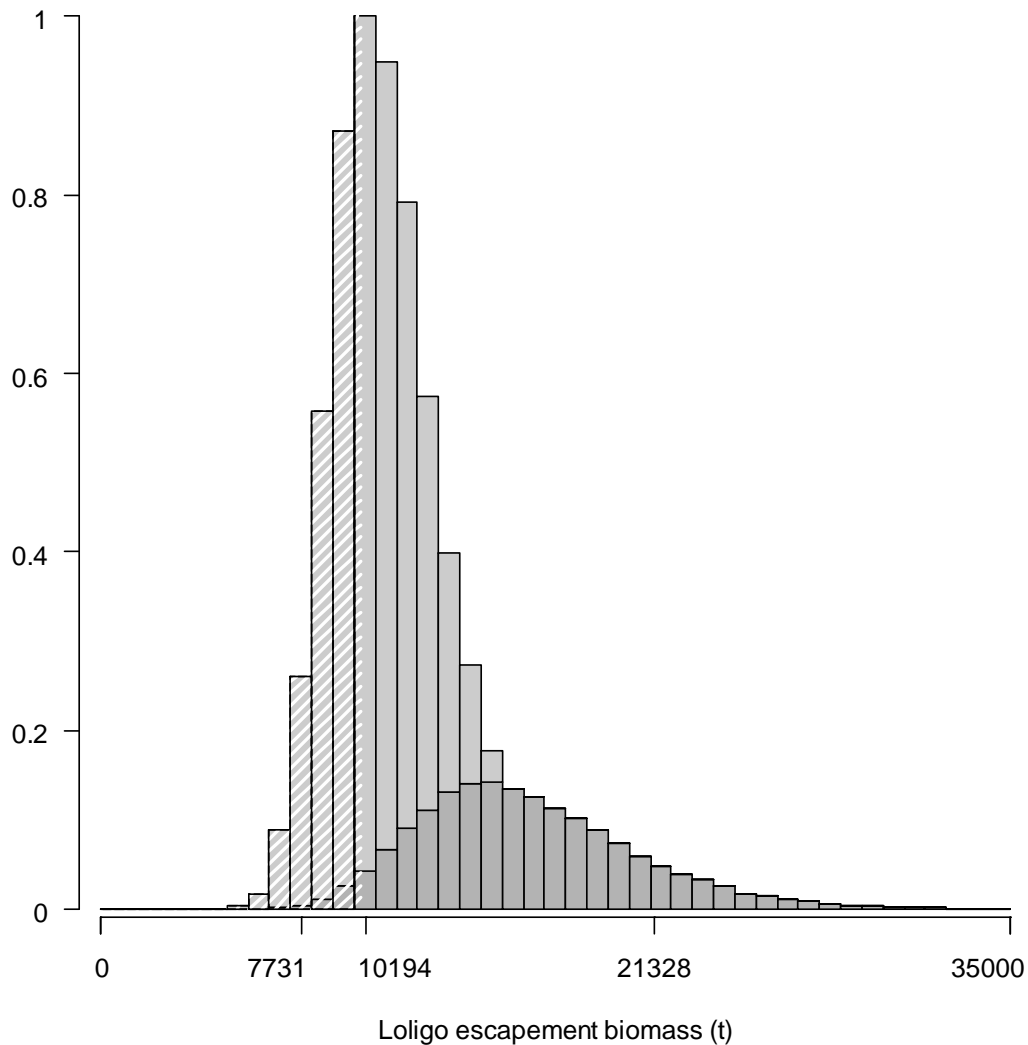


Figure 9. Likelihood distribution with 95% confidence intervals of total *Loligo* escapement biomass corresponding to the season end (April 23rd). White shading lines: portion of the distribution < 10,000 tonnes.


**Immigration**

*Loligo* immigration during the season was inferred on each day by how many more *Loligo* were estimated present than the day before, minus the number caught and the number expected to have died naturally:

$$\text{Immigration } N_{\text{day i}} \quad = \quad N_{\text{day i}} - (N_{\text{day i-1}} - C_{\text{day i-1}} - M_{\text{day i-1}})$$

where $N_{\text{day i-1}}$ are optimized in the depletion models, $C_{\text{day i-1}}$ calculated as in equation 3, and $M_{\text{day i-1}}$ is:

$$M_{\text{day i-1}} \quad = \quad (N_{\text{day i-1}} - C_{\text{day i-1}}) \times (1 - e^{-M})$$

Immigration biomass per day was then calculated as the immigration number per day multiplied by predicted average individual weight from the GAM:

$$\text{Immigration}\,B_{\text{day i}} \quad = \quad \text{Immigration}\,N_{\text{day i}} \times \text{GAM}\,Wt_{\text{day i}}$$

All numbers N are themselves derived from the daily average individual weights, so the estimation factors in that those *Loligo* immigrating on a day would likely be smaller than average. Confidence intervals of the immigration estimates were calculated by applying the above algorithms to the MCMC iterations of the depletion models. Resulting total biomasses of *Loligo* immigration north and south, up to day 111, the last day of *Loligo* target allocation, were:

$$\text{Immigration}\,B_{\text{N day 55-111}} \quad = \quad 3{,}615\,t \sim 95\%\ \text{CI}\ [0-9{,}806]\,t \qquad \textbf{(12-N)}$$

$$\text{Immigration}\,B_{\text{S day 55-111}} \quad = \quad 12{,}411\,t \sim 95\%\ \text{CI}\ [4{,}578-34{,}089]\,t \qquad \textbf{(12-S)}$$

Total immigration with semi-randomized addition of the confidence intervals was:

$$\text{Immigration}\,B_{\text{Total 55-111}} \quad = \quad 16{,}026\,t \sim 95\%\ \text{CI}\ [6{,}068-40{,}379]\,t \qquad \textbf{(12-T)}$$

In the south sub-area, the in-season peaks on days 63, 78 and 95 accounted for 53.3%, 42.5% and 4.2% of in-season immigration (start day 55 was de facto not an in-season immigration), consistent with the variation in the time series biomass shown on Figure 6. In the north sub-area day 71 accounted for all in-season immigration.


**Season schedule extension**

Implementation of the second phase one-week extension of 1st *Loligo* season would normally call for evaluation of the outcome on the *Loligo* stock. However, in this season the outcome has been incomparable due to the extraordinary ingress of *Illex*. In effect, the one-week extension beyond last year's 1st season (Winter, 2014) is exactly the week that was closed to *Loligo* target fishing, from April 22nd to April 28th. Further evaluation of the season schedule changes (Fisheries Committee, 2013) will therefore be deferred until after next season.


**Bycatch**

Of the 871 *Loligo*-target vessel-days in total (Table 1), 225 vessel-days reported a primary catch other than *Loligo*: 221 *Illex*, 3 rock cod (*Patagonotothen ramsayi*) and 1 red cod (*Salilota australis*). The four most common commercial bycatches reported overall for the *Loligo*-target season were *Illex* (8110 t, reported from 345 vessel-days), rock cod (1810 t, 713 vessel-days), red cod (70 t, 41 vessel-days), and blue whiting (*Micromesistius australis*) (15 t, 17 vessel-days). Relative distributions by grid of these bycatches are shown in Figure 10.
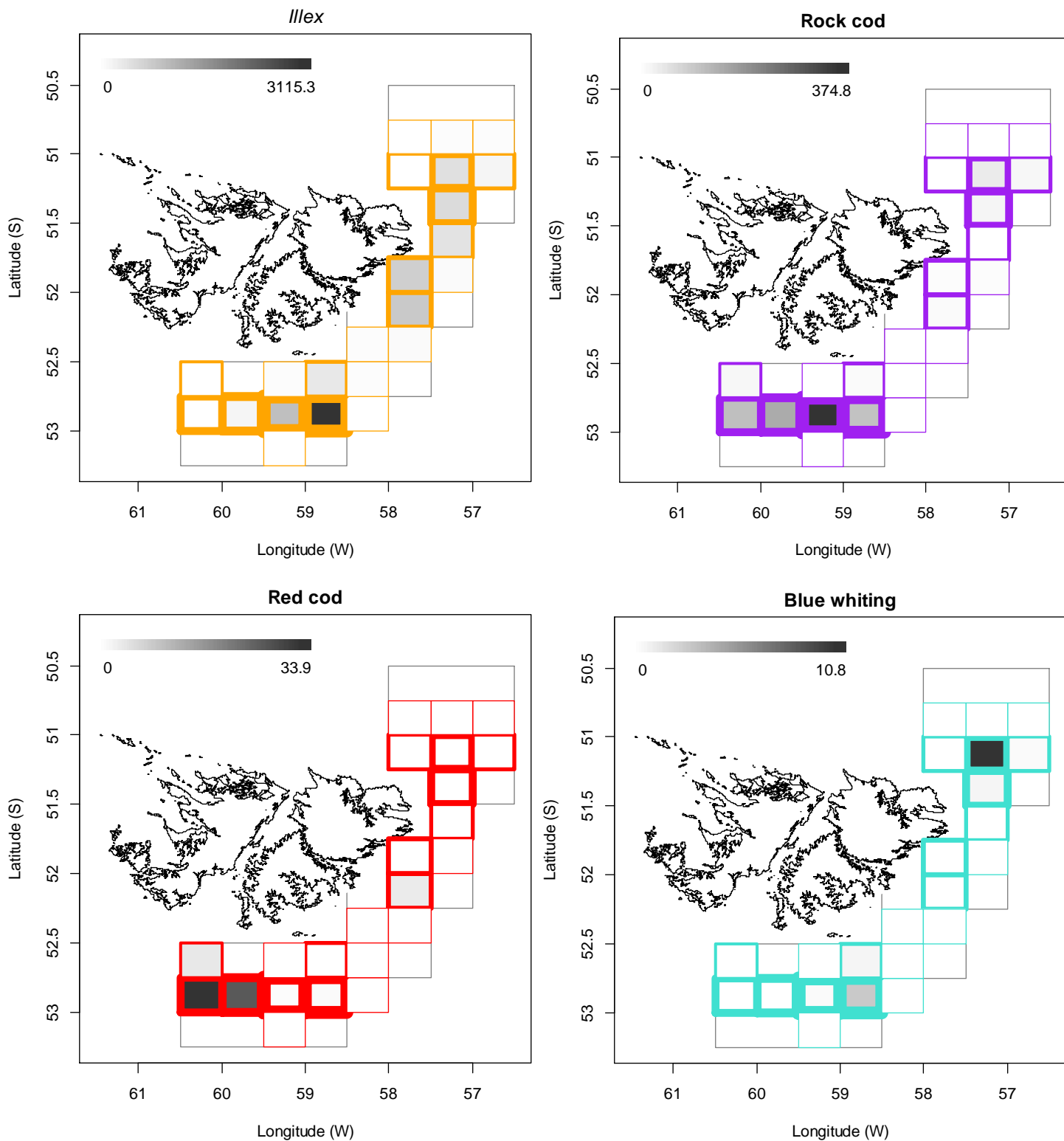
Figure 10. Distributions of the four principal bycatches during 1<sup>st</sup> season 2015. Thickness of grid lines is proportional to the number of vessel-days (1 to 215). Gray-scale is proportional to the bycatch biomass; maximum (tonnes) indicated on each plot.

## References

Agnew, D.J., Baranowski, R., Beddington, J.R., des Clers, S., Nolan, C.P. 1998. Approaches to assessing stocks of *Loligo gahi* around the Falkland Islands. Fisheries Research 35:155-169.

Agnew, D. J., Beddington, J. R., and Hill, S. 2002. The potential use of environmental information to manage squid stocks. Canadian Journal of Fisheries and Aquatic Sciences, 59: 1851–1857.

Arkhipkin, A.I., Middleton, D.A.J. 2002a. Inverse patterns in abundance of *Illex argentinus* and *Loligo gahi* in Falkland waters: possible interspecific competition between squid? Fisheries Research 59:181-196.

Arkhipkin, A.I., Middleton, D.A.J. 2002b. Sexual segregation in ontogenetic migrations by the squid *Loligo gahi* around the Falkland Islands. Bulletin of Marine Science 71: 109-127.

Arkhipkin, A.I., Middleton, D.A.J., Barton, J. 2008. Management and conservation of a short-lived fishery resource: *Loligo gahi* around the Falkland Islands. American Fisheries Society Symposium 49:1243-1252.

Barton, J. 2002. Fisheries and fisheries management in Falkland Islands Conservation Zones. Aquatic Conservation: Marine and Freshwater Ecosystems 12: 127–135.

Brooks, S.P., Gelman, A. 1998. General methods for monitoring convergence of iterative simulations. Journal of computational and graphical statistics 7:434-455.

DeLury, D.B. 1947. On the estimation of biological populations. Biometrics 3:145-167.

Fisheries Committee. 2013. Re-allocation of fishing effort between 1st and 2nd *Loligo* seasons. Proposal to the Fisheries Committee, December 2013. 4 p.

Gamerman, D., Lopes, H.F. 2006. Markov Chain Monte Carlo. Stochastic simulation for Bayesian inference. 2nd edition. Chapman & Hall/CRC.

Magnusson, A., Punt, A., Hilborn, R. 2013. Measuring uncertainty in fisheries stock assessment: the delta method, bootstrap, and MCMC. Fish and Fisheries 14: 325-342.

Nash, J.C., Varadhan, R. 2011. optimx: A replacement and extension of the optim() function. R package version 2011-2.27. http://CRAN.R-project.org/package=optimx

Patterson, K.R. 1988. Life history of Patagonian squid *Loligo gahi* and growth parameter estimates using least-squares fits to linear and von Bertalanffy models. Marine Ecology Progress Series 47:65-74.

Payá, I. 2010. Fishery Report. *Loligo gahi*, Second Season 2009. Fishery statistics, biological trends, stock assessment and risk analysis. Technical Document, Falkland Islands Fisheries Department. 54 p.

Punt, A.E., Hilborn, R. 1997. Fisheries stock assessment and decision analysis: the Bayesian approach. Reviews in Fish Biology and Fisheries 7:35-63.

Roa-Ureta, R. 2012. Modelling in-season pulses of recruitment and hyperstability-hyperdepletion in the *Loligo gahi* fishery around the Falkland Islands with generalized depletion models. ICES Journal of Marine Science 69: 1403–1415.

Roa-Ureta, R., Arkhipkin, A.I. 2007. Short-term stock assessment of *Loligo gahi* at the Falkland Islands: sequential use of stochastic biomass projection and stock depletion models. ICES Journal of Marine Science 64:3-17.

Rosenberg, A.A., Kirkwood, G.P., Crombie, J.A., Beddington, J.R. 1990. The assessment of stocks of annual squid species. Fisheries Research 8:335-350.

Shaw, P.W., Arkhipkin, A.I., Adcock, G.J., Burnett, W.J., Carvalho, G.R., Scherbich, J.N., Villegas, P.A. 2004. DNA markers indicate that distinct spawning cohorts and aggregations of Patagonian squid, *Loligo gahi*, do not represent genetically discrete subpopulations. Marine Biology, 144: 961-970.

Winter, A., Arkhipkin, A. 2012. Predicting recruitment pulses of Patagonian squid in the Falkland Islands fishery. World Fisheries Congress, Edinburgh, Scotland.

Winter, A. 2011. *Loligo gahi* stock assessment, first season 2011. Technical Document, Falkland Islands Fisheries Department. 23 p.

Winter, A. 2013. *Loligo* stock assessment, first season 2013. Technical Document, Falkland Islands Fisheries Department. 23 p.

Winter, A. 2014. *Loligo* stock assessment, first season 2014. Technical Document, Falkland Islands Fisheries Department. 30 p.

Winter, A., Jones, J., Shcherbich, Z. 2015. *Loligo* stock assessment survey, 1st season 2015. Technical Document, Falkland Islands Fisheries Department. 16 p.

## Appendix
## *Loligo* individual weights

A generalized additive model (GAM) was calculated from the daily observer data (both sexes combined) and commercial size category data of average individual daily weights of *Loligo*. North and south sub-areas were calculated separately. For continuity, the GAMs were calculated using all pre-season survey and in-season data contiguously. GAM plots of the north and south sub-areas are shown in Figure A1.
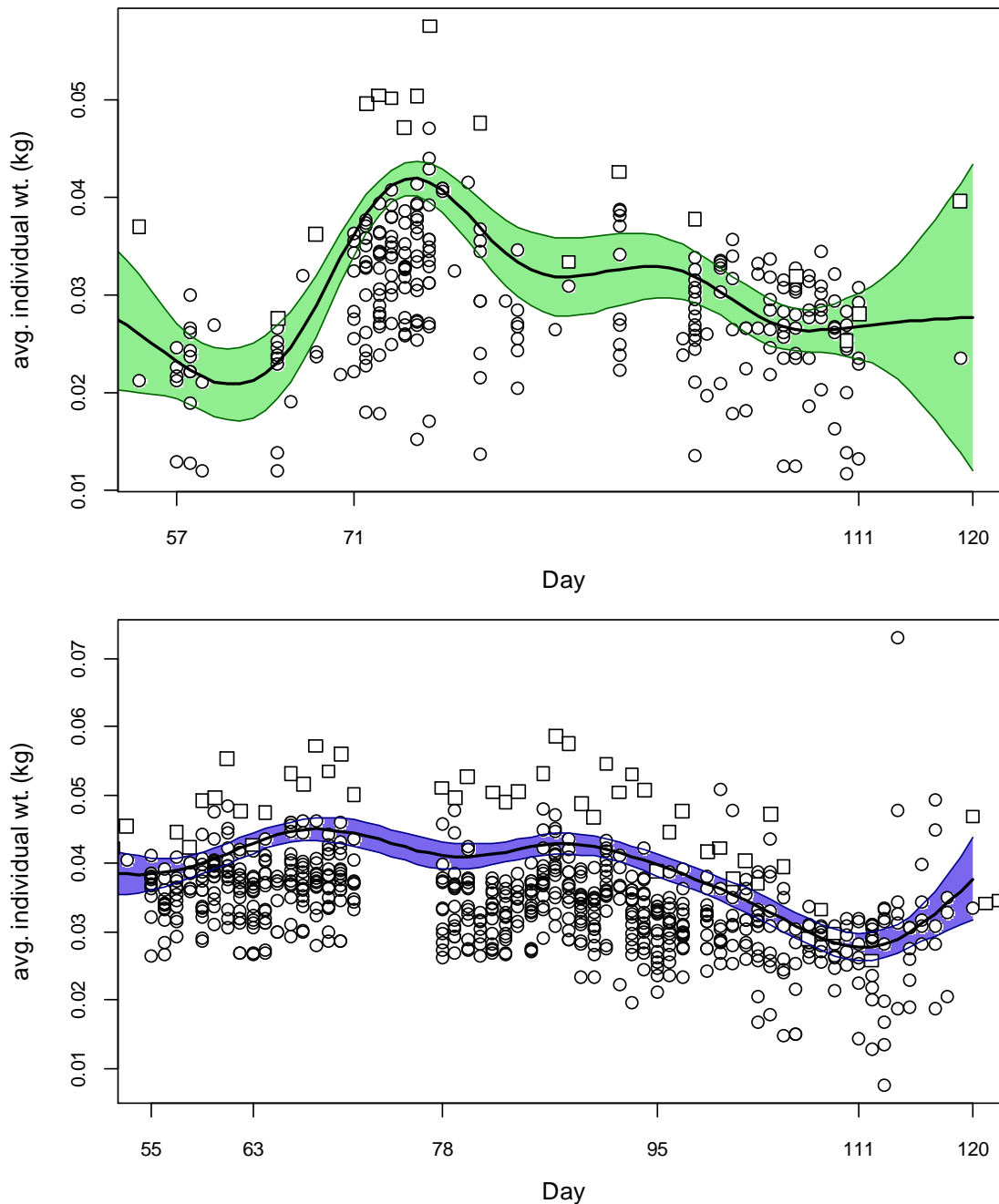


Figure A1. North (top) and south (bottom) sub-area daily average individual *Loligo* weights from commercial size categories per vessel (circles) and observer measurements (squares). GAMs of the daily trends ± 95% confidence intervals (centre lines and colour under-shading).

**Prior estimates and CV**

The pre-season survey (Winter et al., 2015) had estimated *Loligo* biomasses of 7,444 t (standard deviation: ± 1,547 t) north of 52º S and 28,979 t (standard deviation: 3,086 t) south of 52º S. From modelled survey catchability, Payá (2010) had estimated average net escapement of up to 22%, which was added to the standard deviation:

$$7{,}444 \pm \left( \frac{1{,}547}{7{,}444} + .22 \right) \;=\; 7{,}444 \pm 42.8\% \qquad = \quad 7{,}444 \pm 3{,}185 \text{ t.} \qquad \textbf{(A1-N)}$$

$$28{,}979 \pm \left( \frac{3{,}086}{28{,}979} + .22 \right) \;=\; 28{,}979 \pm 32.7\% \qquad = \quad 28{,}979 \pm 9{,}462 \text{ t.} \qquad \textbf{(A1-S)}$$

The 22% was added as a linear increase in the variability, but was not used to reduce the total estimate, because *Loligo* that escape one trawl are likely to be part of the biomass concentration that is available to the next trawl.

*Loligo* numbers at the start of the season, day 55, were estimated as the survey biomasses divided by the GAM-predicted average individual weights on day 55: 0.025 kg north and 0.038 kg south (Figure A1). Coefficients of variation (CV) of the GAM on day 55 were 10.71% north and 3.12% south, and CV of the length-weight conversion relationship (equation **8**) was 7.3%. Combining all sources of variation with the pre-season survey biomass estimates and average individual weights gave estimated *Loligo* numbers at season start (February 24th; day 55) of:

$$_{\text{prior}} N_{\text{N day 55}} \;=\; \frac{7{,}444 \times 1000}{0.025} \pm \sqrt{42.8\%^{\,2} + 10.71\%^{\,2} + 7.3\%^{\,2}}$$

$$= \; 0.296 \times 10^{9} \; \pm \; 44.7\% \qquad\qquad \textbf{(A2-N)}$$

$$_{\text{prior}} N_{\text{S day 55}} \;=\; \frac{28{,}979 \times 1000}{0.038} \pm \sqrt{32.7\%^{\,2} + 3.12\%^{\,2} + 7.3\%^{\,2}}$$

$$= \; 0.754 \times 10^{9} \pm 33.6\% \qquad\qquad \textbf{(A2-S)}$$

The catchability coefficient (q) prior for the north sub-area was taken on day 57, when 5 vessels were fishing north and the first depletion period north started. The abundance (N) on day 57 was calculated as the abundance on start day 55 discounted for 2 days of natural mortality (given that no catch had been taken in those 2 days):

$$_{\text{prior}} N_{\text{N day 57}} \;=\; {}_{\text{prior}} N_{\text{N day 55}} \times e^{-M \cdot (57 - 55)} \;=\; 0.288 \times 10^{9} \qquad \textbf{(A3-N)}$$

$$
\begin{aligned}
_{\text{prior}} q_{\text{ N}} \quad &= \; C(N)_{\text{N day 57}} / ( {}_{\text{prior}} N_{\text{N day 57}} \times E_{\text{N day 57}} ) \\
&= \; (C(B)_{\text{N day 57}} / Wt_{\text{N day 57}}) / ( {}_{\text{prior}} N_{\text{N day 57}} \times E_{\text{N day 57}} ) \\
&= \; (110.6 \text{ t} / 0.023 \text{ kg}) / (0.288 \times 10^{9} \times 5 \text{ vessel-days}) \\
&= \; \textcolor{red}{3.300 \times 10^{-3} \text{ vessels}^{-1} \text{ }^{\text{B}}} \qquad\qquad \textbf{(A4-N)}
\end{aligned}
$$

---

[B] On Figure 7-left.

The catchability coefficient (q) prior for the south sub-area was taken on day 55, when 13 vessels were fishing south. As this was the first scheduled day of the season, no discount was applicable for either natural mortality or catch.

$$
\begin{aligned}
{}_{\text{prior}}q_{\,S} \quad &= \quad C(N)_{\text{S day 55}} / ({}_{\text{prior}}N_{\text{S day 55}} \times E_{\text{S day 55}}) \\
&= \quad (C(B)_{\text{S day 55}} / Wt_{\text{S day 55}}) / ({}_{\text{prior}}N_{\text{S day 55}} \times E_{\text{S day 55}}) \\
&= \quad (398.5 \text{ t} / 0.038 \text{ kg}) / (0.754 \times 10^9 \times 13 \text{ vessel-days}) \\
&= \quad {\color{red}1.058 \times 10^{-3} \text{ vessels}^{-1}}^{\text{ C}}
\end{aligned}
\qquad \textbf{(A4-S)}
$$

CVs of the priors were calculated as the sums of variability in ${}_{\text{prior}}N$ (equations **A2**) plus variability in the catches of vessels on the start days (day 57 N and day 55 S):

$$
CV_{\text{prior N}} \quad = \quad \sqrt{44.7\%^2 + \left( \frac{SD\left(C(B)_{\text{N vessels day 57}}\right)}{\text{mean}\left(C(B)_{\text{N vessels day 57}}\right)} \right)^2}
$$

$$
= \quad \sqrt{44.7\%^2 + 33.0\%^2} \qquad = \quad 55.5\% \qquad \textbf{(A5-N)}
$$

$$
CV_{\text{prior S}} \quad = \quad \sqrt{33.6\%^2 + \left( \frac{SD\left(C(B)_{\text{S vessels day 55}}\right)}{\text{mean}\left(C(B)_{\text{S vessels day 55}}\right)} \right)^2}
$$

$$
= \quad \sqrt{33.6\%^2 + 32.1\%^2} \qquad = \quad 46.5\% \qquad \textbf{(A5-S)}
$$

### Depletion model estimates and CV

For the north sub-area, the equivalent of equation **3** with two $N_{\text{day}}$ was optimized on the difference between predicted catches and actual catches (equation **4**), resulting in parameters values:

$$
\begin{aligned}
{}_{\text{depletion}}N1_{\text{N day 57}} \quad &= \quad 0.471 \times 10^9; \qquad\qquad {}_{\text{depletion}}N2_{\text{N day 71}} \quad = \quad 0.049 \times 10^9 \\[4pt]
{}_{\text{depletion}}q_{\text{N lo }\textit{Illex}} \quad &= \quad {\color{blue}2.037 \times 10^{-3} \text{ vessels}^{-1}}^{\text{ B}} \\
{}_{\text{depletion}}q_{\text{N hi }\textit{Illex}} \quad &= \quad 0.585 \times 10^{-3} \text{ vessels}^{-1} \\[4pt]
{}_{\text{depletion}}q\,\text{switch}_{\text{N}} \quad &= \quad 0.821
\end{aligned}
\qquad \textbf{(A6-N)}
$$

The root-mean-square deviation of predicted vs. actual catches was calculated as the CV of the model:

$$
CV_{\text{rmsd N}} \quad = \quad \frac{\sqrt{\sum_{i=1}^{n}\left({}_{\text{predicted}}C(N)_{\text{N day i}} - {}_{\text{actual}}C(N)_{\text{N day i}}\right)^2 / n}}{\text{mean}\left({}_{\text{actual}}C(N)_{\text{N day i}}\right)}
$$

---

C On Figure 5-left.

$$= 2.524 \times 10^6 \,/\, 4.074 \times 10^6 \;=\; 61.9\% \qquad\qquad \textbf{(A7-N)}$$

Error due to average individual weight estimation was inferred by selecting a random normal value for each day's weight average (mean = GAM predicted mean, s.d. = GAM s.d.; Figure A1-north), then using this vector of randomized average individual weights to re-calculate catch numbers per day and the depletion optimization. This randomization was iterated 1000×. The ratio of standard deviation over mean of the vector of randomized q (lo *Illex*) was calculated as the CV due to individual weight estimation error:

$$\text{CV}_{\text{error Wt N}} \qquad = \quad \frac{\text{sd}\left(q_{\text{rnorm N lo Illex}}\right)}{\text{mean}\left(q_{\text{rnorm N lo Illex}}\right)} \qquad = \; 36.5\% \qquad \textbf{(A8-N)}$$

CVs of the depletion were then calculated as the sum:

$$\text{CV}_{\text{depletion N}} \qquad = \quad \sqrt{\text{CV}_{\text{rmsd N}}{}^2 + \text{CV}_{\text{optim Wt N}}{}^2} \;=\; \sqrt{61.9\%^2 + 36.5\%^2}$$
$$= \; 71.9\% \qquad\qquad \textbf{(A9-N)}$$

For the south sub-area, the equivalent of equation **3** with four $N_{\text{day}}$ was optimized on the difference between predicted catches and actual catches (equation **4**), resulting in parameters values:

| | | | |
|---|---|---|---|
| depletion $N1_{\text{S day 55}}$ | $= 0.254 \times 10^9$; | depletion $N2_{\text{S day 63}}$ | $= 0.077 \times 10^9$ |
| depletion $N3_{\text{S day 78}}$ | $= 0.175 \times 10^9$; | depletion $N4_{\text{S day 95}}$ | $= 0.044 \times 10^9$ |

depletion $q_{\text{S lo Illex}}$      $= 3.166 \times 10^{-3}$ vessels$^{-1}$ [D]
depletion $q_{\text{S hi Illex}}$      $= 0.711 \times 10^{-3}$ vessels$^{-1}$

depletion $q$ switch $_{\text{S}}$      $= 0.754$                       **(A6-S)**

The normalized root-mean-square deviation of predicted vs. actual catches was calculated as the CV of the model:

$$\text{CV}_{\text{rmsd S}} \qquad = \quad \frac{\sqrt{\sum_{i=1}^{n}\left({}_{\text{predicted}}C(N)_{\text{S day i}} - {}_{\text{actual}}C(N)_{\text{S day i}}\right)^2 / n}}{\text{mean}\left({}_{\text{actual}}C(N)_{\text{S day i}}\right)}$$

$$= 1.594 \times 10^6 \,/\, 5.512 \times 10^6 \;=\; 28.9\% \qquad \textbf{(A7-S)}$$

Error due to average individual weight estimation was inferred by selecting a random normal value for each day's weight average (mean = GAM predicted mean, s.d. = GAM s.d.; Figure A1-south), then using this vector of randomized average individual weights to re-calculate catch numbers per day and the depletion optimization. This randomization was iterated 1000×. The ratio of standard deviation over mean of the

---

[D] Off the scale on Figure 5-left.

vector of randomized q (lo *Illex*) was calculated as the CV due to individual weight estimation error:

$$CV_{error\ Wt\ S} \quad = \quad \frac{sd\left(q_{rnorm\ S\ lo\ Illex}\right)}{mean\left(q_{rnorm\ S\ lo\ Illex}\right)} \quad = \quad 28.2\% \qquad \textbf{(A8-S)}$$

CVs of the depletion were then calculated as the sum:

$$CV_{depletion\ S} \quad = \quad \sqrt{CV_{rmsd\ S}^{\ 2} + CV_{optim\ Wt\ S}^{\ 2}} \quad = \quad \sqrt{28.9\%^{\,2} + 28.2\%^{\,2}}$$
$$= \quad 40.4\% \qquad \textbf{(A9-S)}$$

### Combined Bayesian models

For the north sub-area, the joint optimization of equations **4** and **5** resulted in parameters values:

$depletion\ N1_{N\ day\ 57} \quad = 0.258 \times 10^{9};$ $\qquad depletion\ N2_{N\ day\ 71} \quad = 0.120 \times 10^{9}$

$depletion\ q_{N\ lo\ Illex} \quad = 3.306 \times 10^{-3}\ vessels^{-1\ B}$
$depletion\ q_{N\ hi\ Illex} \quad = 0.887 \times 10^{-3}\ vessels^{-1}$

$depletion\ q\ switch_{N} \quad = 0.818^{\,E} \qquad \textbf{(A10-N)}$



**North, two depletion peaks**

---
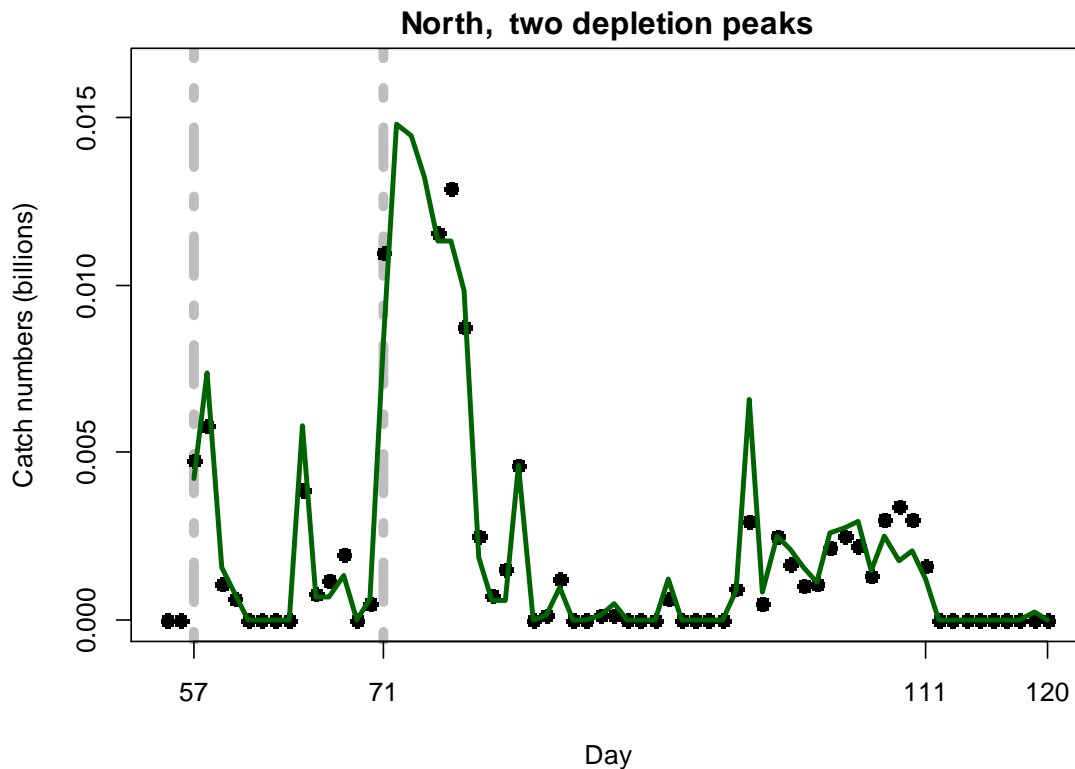
[E] On Figure A3-N.

Figure A2-N [previous page]. Daily catch numbers estimated from actual catch (black points) and predicted from the depletion model (green line) in the north sub-area.

These parameters produced the fit between predicted and actual catches shown in Figure A2-N. The MCMC iterations of the q switch mostly clustered around the optimum of $_{\text{depletion}}\text{q switch}_N = 0.818$, but 22% were < 0.74 (Figure A3-N).
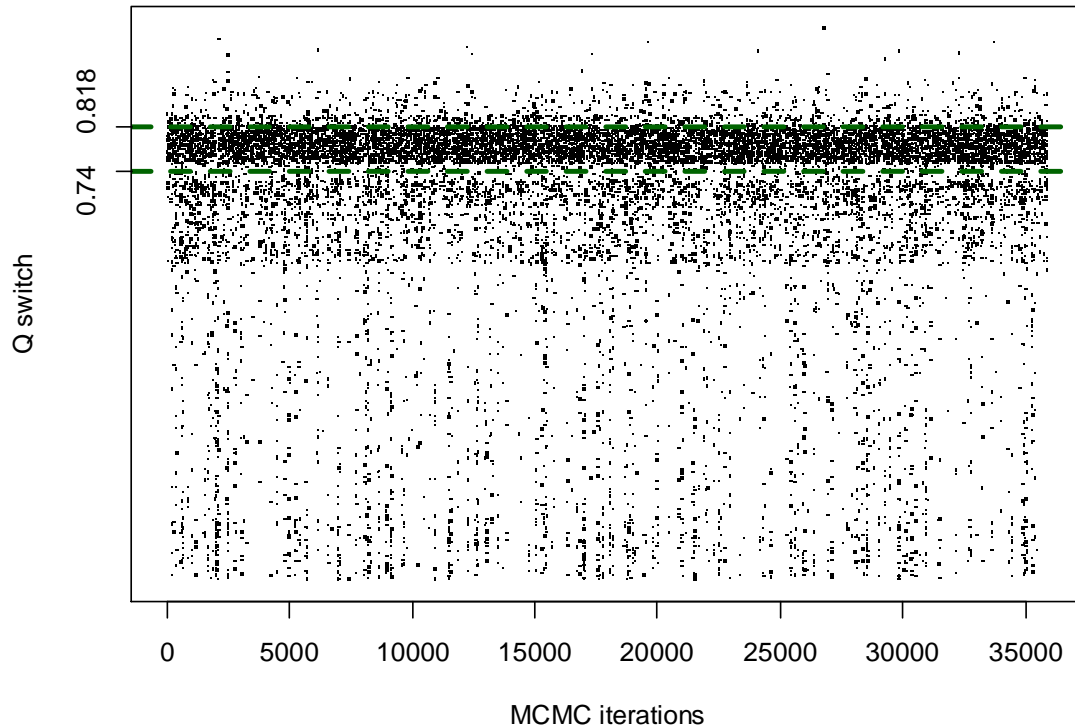


Figure A3-N. North MCMC iterations of the q switch setting the proportion of *Illex* in total squid catch that would trigger a different catchability coefficient q. The two biomass modes in Figure 7-right were calculated using 0.74 as the break.

For the south sub-area, the joint optimization of equations **4** and **5** resulted in parameters values:

$$_{\text{depletion}}\text{N1}_{\text{S day 55}} = 0.668 \times 10^9; \qquad _{\text{depletion}}\text{N2}_{\text{S day 63}} = 0.130 \times 10^9$$

$$_{\text{depletion}}\text{N3}_{\text{S day 78}} = 0.123 \times 10^9; \qquad _{\text{depletion}}\text{N4}_{\text{S day 95}} = 0.040 \times 10^9$$

$$_{\text{depletion}}\text{q}_{\text{S lo }Illex} = 1.114 \times 10^{-3} \text{ vessels}^{-1\text{ C}}$$

$$_{\text{depletion}}\text{q}_{\text{S hi }Illex} = 0.179 \times 10^{-3} \text{ vessels}^{-1}$$

$$_{\text{depletion}}\text{q switch}_S = 0.907^{\text{ F}} \qquad\qquad \textbf{(A10-S)}$$

These parameters produced the fit between predicted and actual catches shown in Figure A2-S. The MCMC iterations of the q switch mostly clustered around the optimum of $_{\text{depletion}}\text{q switch}_S = 0.907$, but 21% were < 0.82 (Figure A3-S).

---

[F] On Figure A3-S.
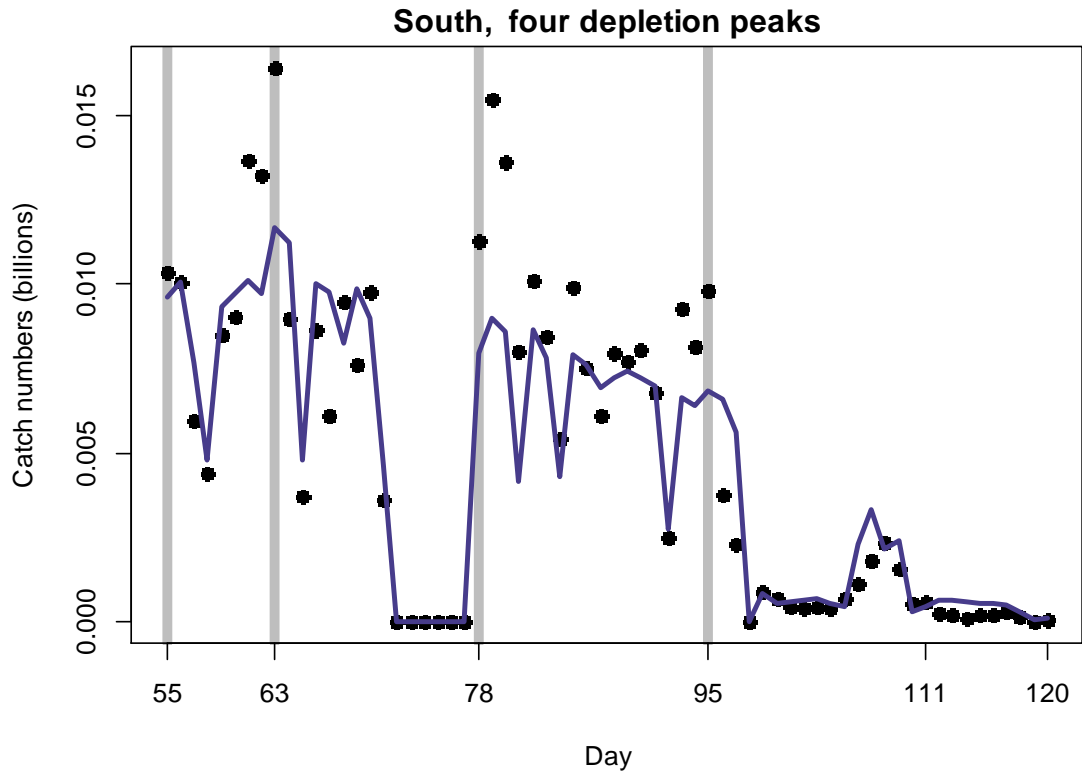
**South, four depletion peaks**

Figure A2-S. Daily catch numbers estimated from actual catch (black points) and predicted from the depletion model (blue line) in the south sub-area.
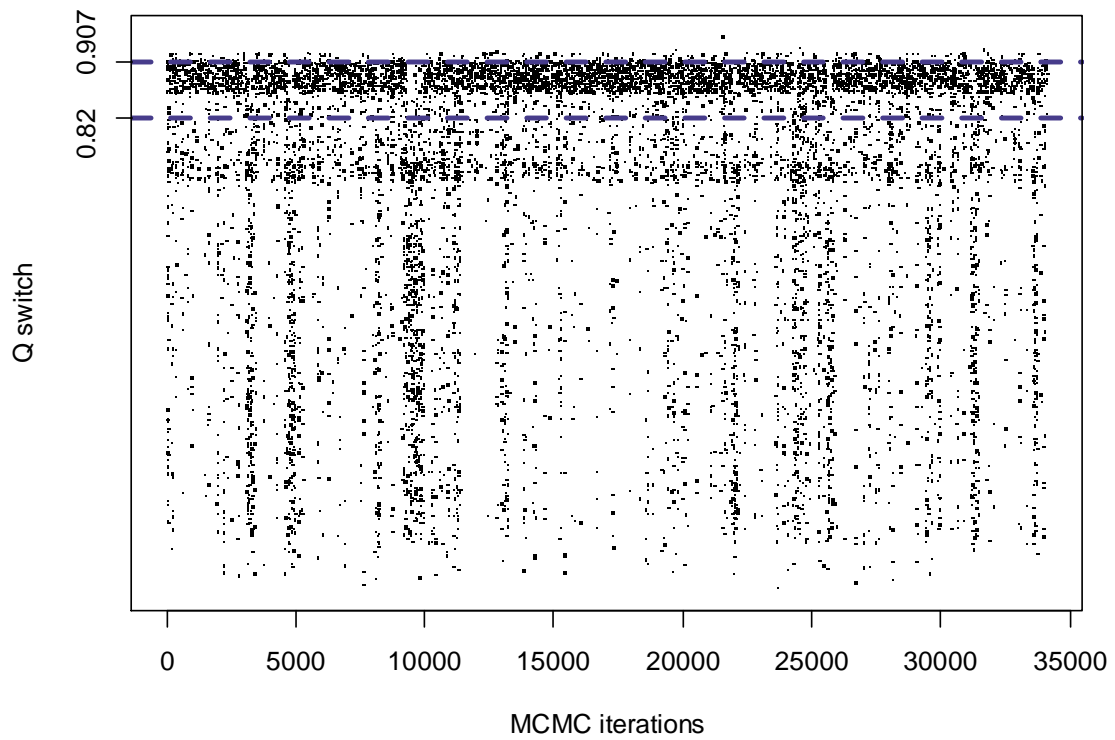


Figure A3-S. South MCMC iterations of the q switch setting the proportion of *Illex* in total squid catch that would trigger a different catchability coefficient q. The two biomass modes in Figure 5-right were calculated using 0.82 as the break.

27

**Semi-randomized addition of north and south likelihood distributions**

North and south biomass time series estimated from depletion models are potentially correlated. In $1^{st}$ season of 2015 the correlation coefficient between north and south biomasses per day (to the season minimum day, April $23^{rd}$) was:

$$r\left(B_{N \text{ day } 55\text{-}113}, B_{S \text{ day } 55\text{-}113}\right) \quad = +0.640 \tag{A11}$$

To incorporate this correlation in the addition of the north and south escapement biomasses, the highest common number of iterations was taken from the respective north and south likelihood distributions (because of the variable MCMC thinning algorithm (see Methods), they were not necessarily identical). These were separately ordered by magnitude of the iterations. Then, each ordered iteration of the south escapement biomass[G] was randomly flagged for either permutation or not, in proportion to the correlation; i.e., each iteration had a 1 - 0.640 = 0.360 probability of being flagged for permutation. Then, the subset of all flagged iterations was randomly permuted. Then, the ordered set of north escapement biomass likelihood iterations, and the ordered, flagged, and partially permuted set of south escapement biomass likelihood iterations, were added together. The process was replicated 7× for greater statistical power.

Limit expectations of this algorithm are that if correlation had been zero, then 1 – 0 = all of the iterations would have been permuted, and the addition of the north and south sets of likelihood iterations would have been fully randomized. If correlation had been 100%, then 1 – 1 = none of the iterations would have been permuted, and the north and south sets of likelihood iterations would have been added together fully ordered; i.e. the smallest value of the north set plus the smallest value of the south set, the $2^{nd}$-smallest value of the north set plus the $2^{nd}$-smallest value of the south set, etc. If the biomass time series correlation $r\left(B_{N \text{ day } 55\text{-}113}, B_{S \text{ day } 55\text{-}113}\right)$ had been negative, then one of the two sets of north or south likelihood iterations would have been reverse-ordered so that their addition would have been back-to-front, notwithstanding the degree of permutation.

For the dual-mode distributions the proportions below and above their respective q breaks (0.74 north and 0.82 south) were correlated and recombined separately.

The same procedure for semi-randomized addition was also applied to the north and south likelihood distributions of immigration biomass.

---

[G] Whereby it is arbitrary whether this was done with the south or north likelihood iterations. What matters is the degree of randomization of one relative to the other.